AIP | Applied Physics Letters

Raman spectroscopy as a probe for the coupling of light into ensembles of sub-wavelength-sized nanowires

C. Pfüller, M. Ramsteiner, O. Brandt, F. Grosse, A. Rathsfeld et al.

Citation: Appl. Phys. Lett. **101**, 083104 (2012); doi: 10.1063/1.4747208
View online: http://dx.doi.org/10.1063/1.4747208
View Table of Contents: http://apl.aip.org/resource/1/APPLAB/v101/i8
Published by the American Institute of Physics.

Raman spectroscopy as a probe for the coupling of light into ensembles of sub-wavelength-sized nanowires

C. Pfüller,[1] M. Ramsteiner,[1] O. Brandt,[1,a)] F. Grosse,[1] A. Rathsfeld,[2] G. Schmidt,[2] L. Geelhaar,[1] and H. Riechert[1]
[1]*Paul-Drude-Institut für Festkörperelektronik, Hausvogteiplatz 5–7, D-10117 Berlin, Germany*
[2]*Weierstraß-Institut für Angewandte Analysis und Stochastik, Mohrenstraße 39, 10117 Berlin, Germany*

(Received 28 June 2012; accepted 6 August 2012; published online 21 August 2012)

We use Raman scattering to investigate how light penetrates into and escapes out of GaN nanowires with diameters and interspacings smaller than the effective wavelength of the light. Quantitatively, the efficiencies for light coupling into and out of the nanowires can be explained by considering the nanowire ensemble as a homogeneous effective medium. The observed phonon modes in the Raman spectra, however, suggest that light enters the nanowires to a considerable extent through their side facets even for normal incidence. This finding is supported by rigorous calculations of the spatially distributed light intensity within a periodic nanowire structure. © *2012 American Institute of Physics*. [http://dx.doi.org/10.1063/1.4747208]

The synthesis of nanowires (NWs) is a promising route to the fabrication of efficient light-emitting diodes (LEDs) as they grow virtually strain-free even on substrates with a high mismatch in lattice constants and thermal expansion coefficients.[1] Their nanometer-sized lateral dimensions allow for the efficient elastic relief of strain[2] and thus the growth of heterostructures with a low density of structural defects.[3] Consequently, NW-based LEDs are considered as potential candidates for future lighting applications. The small diameter of such NWs, however, also poses new challenges. Surface-related phenomena may become dominant in NWs and may considerably alter the optical and electrical properties of NW LEDs.[4–7] Particularly, nonradiative surface recombination may become a major recombination channel[8,9] and surface depletion may impede the transport of charge carriers through NWs altogether.[10]

Another important aspect is the coupling of light with these NWs, whose diameters and interspacings are typically smaller than the effective wavelength of the emitted light. With regard to applications as a light emitter, the extraction efficiency is of particular importance. Consequently, this subject has been approached using various theoretical concepts. Single, freestanding NWs modeled as dielectric cylinders have been demonstrated to lose their capability to guide the fundamental HE_{11} mode for diameters $D < 0.15\lambda$ and radiation thus couples efficiently to free space.[11–13] High density NW ensembles with sub-wavelength dimensions, on the other hand, have been shown to be adequately described by a Maxwell-Garnett effective media approximation, in the frame of which the extraction efficiency has been found to monotonically increase with decreasing fill factor.[14]

Here, we experimentally investigate the coupling and propagation of light within as-grown GaN NW ensembles using Raman scattering. Combined with calculations of the light intensity distribution in these structures, we give quantitative estimates of the efficiencies with which light couples into and out of the NW ensemble. This easy-to-apply method works in the transparent spectral range of the material, does not require any knowledge about its internal quantum efficiency, and is thus ideally suited for the determination of the extraction efficiency of light out of a structure with arbitrary geometry.

GaN NWs were synthesized without any external catalyst by plasma-assisted molecular beam epitaxy. The NWs were grown on Si(111) under N-rich conditions (N/Ga = 1.2). The substrate temperature during growth was 820 °C. A more detailed description of the growth procedure is given elsewhere.[15] The NWs have grown along the *c*-direction with an average length of about 1.6 μm. A histogram of the NW diameters obtained from scanning electron micrographs with a total area of 20 μm^2 is depicted in Fig. 1. From these micrographs, the density of NWs can be estimated to be $4 \times 10^9\,cm^{-2}$. The diameter distribution is described well by a shifted Γ distribution that has its mean at 110 nm and a variance of 50 nm. The fill factor of the ensemble can thus be

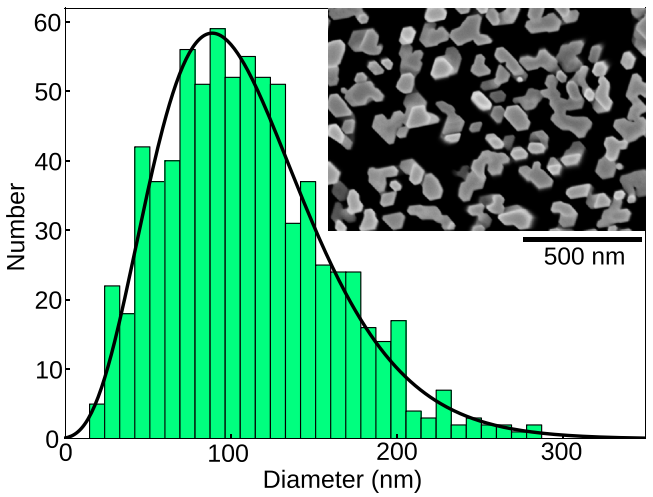

FIG. 1. Histogram of the NW diameter. The solid line depicts a fit to the experimental diameter distribution with a Γ distribution. Inset: Top-view scanning electron micrograph of the GaN NW ensemble.

a)Author to whom correspondence should be addressed. Electronic mail: brandt@pdi-berlin.de.

determined to be 0.38. A large number of NWs has undergone coalescence with neighboring NWs, as evident from the inset of Fig. 1, explaining the large variation in diameter which ranges from 20 to 250 nm. Uncoalesced NWs exhibit a hexagonal cross section with atomically flat *M*-plane sidewalls and a *C*-plane top facet. The GaN reference layer was grown along the *c*-axis by metal-organic chemical vapor deposition on Si(111). It has a thickness of 1.59 μm, is free of cracks, and exhibits a surface roughness of less than 0.3 nm over an area of $5 \times 5\ \mu m^2$.

Raman measurements of the GaN NW ensemble and the GaN layer were performed at room temperature in backscattering geometry such that the *z*-direction is oriented parallel to the NWs' *c*-axis. The 413.1 and 482.5-nm lines of a Coherent Kr^+ ion laser were focused onto the sample by a confocal microscope using objectives whose numerical aperture (NA) ranged from 0.24 to 0.9. The diameter of the excitation and collection area decreased with increasing NA from 10 to 1 μm. The scattered signal was collected by the same objective and dispersed spectrally by a grating with 2400 lines/mm located in an 80-cm Jobin-Yvon monochromator. The signal was recorded using a LN_2-cooled CCD. The polarization of the incoming light was varied by a Fresnel rhomb. A linear polarizer was used to analyze the polarization of the scattered signal. In the polarized configuration $[z(y,y)\bar{z}]$, the polarization direction of the incoming laser light and that of the analyzer are in parallel, while in the depolarized configuration $[z(x,y)\bar{z}]$, they are oriented perpendicularly to each other. The spectral resolution of the setup is about 1 cm^{-1}. The inset of Fig. 2 depicts the geometry of the Raman measurements. In order to measure the intensity of the reflected/scattered signal, the linearly polarized components of the incoming and outgoing light has been converted into circularly polarized components using a $\lambda/4$ plate.

Figure 2 displays polarized $[z(y,y)\bar{z}]$ and depolarized $[z(x,y)\bar{z}]$ Raman spectra of the GaN NW ensemble and of the GaN layer. For wavenumbers larger than 600 cm^{-1}, the signal is enlarged by a factor of 15 in order to visualize the

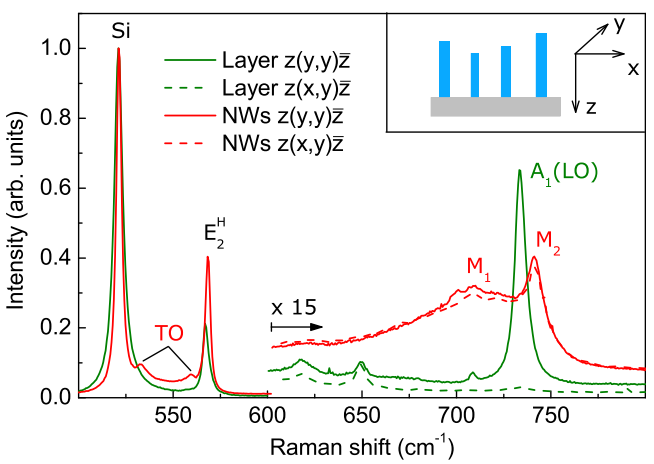

FIG. 2. Raman spectrum of a GaN layer (green) and a GaN NW ensemble (red), both grown on Si. The spectra are normalized to the intensity of the Si optical phonon which originates from the substrate. For wavenumbers larger than 600 cm^{-1}, the signal is enlarged by a factor of 15. The spectra shown are recorded using the 413.1-nm line of the Kr^+ ion laser, but essentially identical ones are obtained with the 482.5-nm line. The inset depicts the geometry of the setup.

LO phonon part of the spectra. All spectra are dominated by the optical phonon peak from the Si substrate at 521.0 cm^{-1}.[16] In the polarized configuration, the spectrum of the layer exhibits the E_2^H phonon at 567.2 cm^{-1} and the A_1(LO) phonon at 733.5 cm^{-1}.[17] The E_2^H frequency indicates the presence of a small tensile strain in the GaN layer. As expected from the selection rules for hexagonal GaN,[17] the A_1(LO) is not observed in the depolarized configuration. The NWs exhibit a slightly higher frequency of the E_2^H phonon at 568.4 cm^{-1} essentially corresponding to that of unstrained GaN. The LO phonon part of the spectrum of the NWs differs considerably from that of the layer. At the position of the A_1(LO) phonon, no peak is observed. Instead, a broad band (M_1) centered at about 708 cm^{-1} as well as a narrow peak (M_2) at 741.2 cm^{-1} are found. Both of these features do not exhibit a marked polarization dependence.

The broad low-frequency peak (M_1) is commonly assigned to surface-optical (SO) phonon modes described by a model which considers the NWs as isolated dielectric cylinders.[18–20] Their interaction with electromagnetic waves is treated by taking into account the dielectric function of the bulk material and the boundary conditions of the electric field at the interface of the nanostructure with the surrounding environment. Within this model, SO phonon modes are sustained at frequencies for which the amplitude of the propagating wave decays rapidly with the distance to the surface. Their frequencies depend on the nanostructure shape, size, and the dielectric constant of the surrounding medium. For the present case and the mean diameter of 110 nm determined in Fig. 1, the M_1 mode is expected to occur at 710 cm^{-1}, i.e., close to the experimental one, when assuming that the mode is predominantly of E_1 symmetry.

Recently, an alternative approach has been proposed to explain the origin of the phonon modes M_1 and M_2 in subwavelength NW ensembles.[21,22] The NW ensemble is considered to represent a homogeneous effective medium with the interaction between NWs and electromagnetic waves described by the definition of an appropriate effective dielectric function. The so-called Fröhlich phonon modes are then obtained as poles and zeros in the effective dielectric function that do not have their counterpart in bulk material. In contrast to the common SO phonon approach described above, these characteristic frequencies [Eqs. (8) to (10) in Ref. 21] depend essentially on the fill factor of the ensemble and not on the NWs' diameter or shape. Using the Maxwell-Garnett effective medium approximation with the present fill factor of 0.38, the M_1 mode is expected to occur at 703 cm^{-1}, again close to the experimental position.

The interpretation of the Raman spectra in the framework of an effective medium approximation is attractive as it allows us to obtain a quantitative estimate of the efficiency with which light couples to our GaN NW ensemble in comparison to the GaN layer. For this purpose, we use the integrated intensity I_R of the E_2^H bulk-phonon mode (sum of polarized and depolarized Raman signals) obtained from side-by-side measurements of the GaN layer and the GaN NW ensemble. The expected relative intensities are determined by using the formalism for the calculation of the Raman signal from a thin film on a thick substrate described in Ref. 23. This formalism takes into account absorption,

multiple reflections, and interference effects. We assume a perfect backscattering configuration since our experimental results are nearly independent of the numerical aperture (between 0.24 and 0.9) of the microscope objectives used for the Raman measurements. For the complex refractive indices of GaN and Si, we use the values $n_{GaN} = 2.54$ (2.46) and $n_{Si} = 5.22 + 0.27i$ $(4.40 + 0.083i)$ at a wavelength of 413.1 (482.5) nm. The NW ensemble is regarded as a homogeneous effective medium with a refractive index of $n_{NW} = 1.33(1.32)$ for the given fill factor in the Maxwell-Garnett approximation.[14] Furthermore, the finite distribution of the NW length has been taken into account by averaging the result for layer thicknesses between 1550 and 1650 nm.

As a result of these calculations, the ratio between the Raman intensities from the NW ensemble and GaN layer is determined to be 3.73 (4.16) at a wavelength of 413.1 (482.5) nm. Experimentally, I_R was found to be higher for the NWs than for the layer, typically by a factor of 1.5, irrespective of the excitation conditions. Since the Raman intensity is proportional to the excited volume, this difference increases to a factor of 3.95 when taking into account the NWs' fill factor of 0.38. Evidently, the theoretical and experimental intensity ratios are in satisfactory agreement, and the description of the NW ensemble as an effective medium thus appears to be a sensible approximation.

Using the same formalism,[23] we next determine the relative efficiencies with which light couples into (η_{in}) and out (η_{out}) of the structure. The overall Raman efficiency is essentially proportional to the product of η_{in} and η_{out}. To decouple these two quantities, we calculate the relative intensities (integrated over the entire layer thickness) of the incident light in the NW ensemble and the GaN layer. The incident intensity is obtained by setting the Raman intensity to unity in the entire layer. As a result, we find η_{in} for the NW ensemble to be larger by a factor of 2.45 (2.54) as compared to the GaN layer. Consequently, η_{out} follows to be larger by factor of 1.52 (1.64) as compared to the GaN layer. The NW geometry thus improves the coupling of incident light into the material (relevant for photovoltaics) as well as the extraction efficiency (the quantity relevant for LEDs).

The effective-medium model used above for the interpretation of the Raman spectra facilitates the straightforward quantitative analysis of Raman intensities. However, we point out that some of our observations cannot be understood in this framework and seem to necessitate a more rigorous theoretical treatment of the light coupling in NW ensembles. Particularly, the frequency of the M_2 phonon mode (cf. Fig. 2) detected from the NW ensemble corresponds exactly to that of the pure E_1(LO) phonon, an observation which holds for a number of different NW samples we have investigated in the course of the present work. This result contradicts the predicted dependence of the M_2 frequency on the fill factor.[21] Note that this dependence was not observed in Ref. 21 either. Together with the observation of A_1(TO) and E_1(TO) phonon modes at 532.5 cm^{-1} and at 559.4 cm^{-1} in the Raman spectra of the NW ensemble, this fact suggests that a considerable amount of light enters and leaves the NWs with wavevectors nearly perpendicular to the NWs' c-axis (see selection rules in Ref. 17). This conclusion is consistent with the work of Lazić *et al.* who suggested the LO mode of InN NWs measured in backscattering geometry to be of E_1 symmetry.[24]

For an understanding of these observations, we recall that the diameter of the majority of the NWs is smaller than the wavelength of the incident light. Qualitatively, an incident plane wave propagating along the z-direction will thus not enter the NWs top facet but will rather be diffracted at the NW tips. The spherical waves emanating from a NW tip will then encounter adjacent NWs from their side. To confirm this qualitative understanding, we calculated the spatial distribution of the light intensity $I = |\vec{E}|^2$ with the electromagnetic field $\vec{E}$ within a periodic array of GaN NWs with sub-wavelength dimensions on a Si substrate.[25,26] To conform to the experimental conditions, we solved the Maxwell equations assuming the incident light to travel as plane wave whose $\vec{k}$-vector points in z-direction. Consequently, the z-component of the electric field E_z of this plane wave equals zero. Figure 3(a) depicts the distribution of E_z^2 within one NW of the periodic array. Close to the NW sidewalls, E_z^2 clearly differs from zero, which is only possible for wave vectors $\vec{k}$ with non-zero components in x- or y-direction. In other words, the direction of the wavevector has changed with respect to that of the incoming light due to diffraction. The observation of $E_z^2 > 0$, thus, directly confirms that the incoming plane wave is diffracted at the NW tips and that light enters sub-wavelength-sized NWs to a considerable amount through their sidewalls, even for light entering the NW ensemble exactly along the z-direction.

Figure 3(b) depicts the distribution of the total intensity of light $I = |\vec{E}|^2 = E_x^2 + E_y^2 + E_z^2$ within a GaN NW. The light forms standing waves inside the NWs, and thus the intensity distribution exhibits a sinusoidal profile along the NW axis, which is caused by reflection at the NW top facet and at the substrate interface. In the present case, the wavelength of the light is set to 482.5 nm. We observed the formation of standing waves for a range of wavelengths, even for light with a wavelength of 325 nm, i.e., in the absorbing

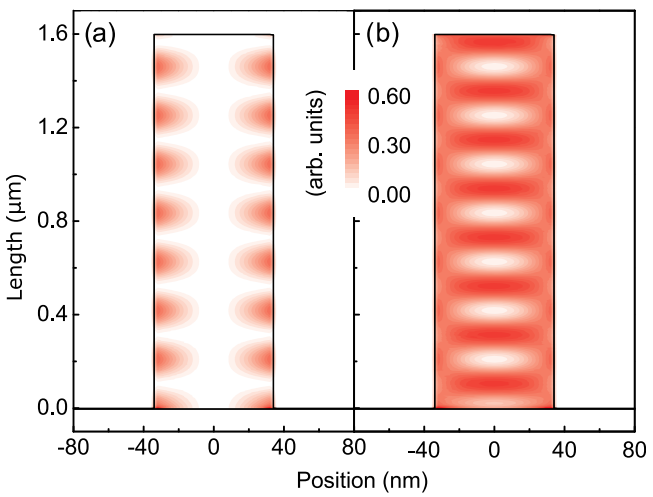

FIG. 3. Intensity distribution within a GaN NW obtained from the solution of the Maxwell equations for a periodic square array of hexagonal NWs standing on a Si substrate. The figures display a cross-section through one unit cell, and the incident light is assumed to have a wavelength of 482.5 nm. (a) Distribution of E_z^2 within a NW, i.e., of light with a wavevector having nonzero in-plane components. (b) Distribution of the total intensity $I = |\vec{E}|^2 = E_x^2 + E_y^2 + E_z^2$ within a NW.

range of GaN. For these wavelengths, the sinusoidal profile is damped such that the amplitude decreases slightly with decreasing distance to the substrate. However, a significant light intensity can be found along the entire NW length. Hence, in optical experiments performed in backscattering geometry such as Raman and photoluminescence (PL) measurements, even NWs vastly exceeding the penetration depth of bulk material (here: 100 nm) are basically excited along their entire length, thanks to the lateral propagation of light.

In summary, we have presented a study of the coupling of light with sub-wavelength-sized GaN NWs based on Raman scattering. Considering the NW ensemble as an effective-medium, we determined η_{in}, the relative efficiency for light coupling into the NWs, as well as η_{out}, the relative extraction efficiency. Both η_{in} and η_{out} of the NW ensemble were found to be about 2 times higher than that of the GaN layer. Qualitatively, we have shown that even for normal incidence, a considerable amount of light couples into and out of NWs through their sidewalls and along their entire length.

We are indebted to Pinar Dogan (PDI) and Philip Drechsel (Osram Opto) for providing the state-of-the-art GaN/Si samples used in this study. A critical reading of the manuscript by Uwe Jahn is gratefully acknowledged.

[1]C. M. Lieber and Z. L. Wang, MRS Bull. **32**, 99 (2007).
[2]A. E. H. Love, *A Treatise on the Mathematical Theory of Elasticity*, 4th ed. (Dover, New York, 1944).
[3]E. P. A. M. Bakkers, M. T. Borgström, and M. A. Verheijen, MRS Bull. **32**, 117 (2007).
[4]R. Agarwal and C. M. Lieber, Appl. Phys. A **85**, 209 (2006).
[5]O. Brandt, C. Pfüller, C. Chèze, L. Geelhaar, and H. Riechert, Phys. Rev. B **81**, 045302 (2010).
[6]C. Pfüller, O. Brandt, F. Grosse, T. Flissikowski, C. Chèze, V. Consonni, L. Geelhaar, H. T. Grahn, and H. Riechert, Phys. Rev. B **82**, 045320 (2010).
[7]R. Calarco, T. Stoica, O. Brandt, and L. Geelhaar, J. Mater. Res. **26**, 2157 (2011).
[8]J. B. Schlager, K. A. Bertness, P. T. Blanchard, L. H. Robins, A. Roshko, and N. A. Sanford, J. Appl. Phys. **103**, 124309 (2008).
[9]P. Parkinson, H. J. Joyce, Q. Gao, H. H. Tan, X. Zhang, J. Zou, C. Jagadish, L. M. Herz, and M. B. Johnston, Nano Lett. **9**, 3349 (2009).
[10]R. Calarco, M. Marso, T. Richter, A. I. Aykanat, R. Meijers, A. V. D. Hart, T. Stoica, and H. Lüth, Nano Lett. **5**, 981(2005).
[11]A. V. Maslov, M. I. Bakunov, and C. Z. Ning, J. Appl. Phys. **99**, 024314 (2006).
[12]T. Voss, G. T. Svacha, E. Mazur, S. Müller, C. Ronning, D. Konjhodzic, and F. Marlow, Nano Lett. **7**, 3675 (2007).
[13]I. Friedler, C. Sauvan, J. P. Hugonin, P. Lalanne, J. Claudon, and J. M. Gérard, Opt. Express **17**, 2095–2110 (2009).
[14]A.-L. Henneghien, G. Torbot, B. Daudin, O. Lartigue, Y. Désières, and J.-M. Gérard, Opt. Express **19**, 527 (2011).
[15]P. Dogan, O. Brandt, C. Pfüller, A.-K. Bluhm, L. Geelhaar, and H. Riechert, J. Cryst. Growth **323**, 418 (2011).
[16]J. H. Parker, Jr., D. W. Feldman, and M. Ashkin, Phys. Rev. **155**, 712–714 (1967).
[17]H. Harima, J. Phys.: Condens. Matter **14**, R967 (2002).
[18]R. Ruppin and R. Englman, Rep. Prog. Phys. **33**, 149 (1970).
[19]M. Watt, C. M. Sotomayor Torres, H. E. G. Arnot, and S. P. Beaumont, Semicond. Sci. Technol. **5**, 285 (1990).
[20]R. Gupta, Q. Xiong, G. D. Mahan, and P. C. Eklund, Nano Lett. **3**, 1745 (2003).
[21]R. Mata, A. Cros, K. Hestroffer, and B. Daudin, Phys. Rev. B **85**, 035322 (2012).
[22]J. Wang, F. Demangeot, R. P'chou, A. Ponchet, A. Cros, and B. Daudin, Phys. Rev. B **85**, 155432 (2012).
[23]M. Ramsteiner, C. Wild, and J. Wagner, Appl. Opt. **28**, 4017 (1989).
[24]S. Lazić, E. Gallardo, J. Calleja, F. Agulló-Rueda, J. Grandal, M. Sánchez-Garcia, E. Calleja, E. Luna, and A. Trampert, Phys. Rev. B **76**, 205319 (2007).
[25]P. Monk, *Finite Element Methods for Maxwell's Equations* (Oxford University Press, Oxford, 2003).
[26]M. Huber, J. Schöberl, A. Sinwel, and S. Zaglmayr, SIAM J. Sci. Comput. **31**, 1500 (2009).